IOP Conf. Series: Materials Science and Engineering **329** (2018) 012012 doi:10.1088/1757-899X/329/1/012012

Optimization of the A-TIG welding for stainless steels

M Jurica, Z Kožuh, I Garašić and M Bušić

University of Zagreb, Faculty of Mechanical Engineering and Naval Architecture, Ivana Lučića 5, 10002 Zagreb, Republic of Croatia

E-mail: matija.busic@fsb.hr

Abstract. The paper presents the influence of the activation flux and shielding gas on tungsten inert gas (A-TIG) welding of the stainless steel. In introduction part, duplex stainless steel was analysed. The A-TIG process was explained and the possibility of welding stainless steels using the A-TIG process to maximize productivity and the cost-effectiveness of welded structures was presented. In the experimental part duplex, 7 mm thick stainless steel has been welded in butt joint. The influence of activation flux chemical composition upon the weld penetration has been investigated prior the welding. The welding process was performed by a robot with TIG equipment. With selected A-TIG welding technology preparation of plates and consumption of filler material (containing Cr, Ni and Mn) have been avoided. Specimens sectioned from the produced welds have been subjected to tensile strength test, macrostructure analysis and corrosion resistance analysis. The results have confirmed that this type of stainless steel can be welded without edge preparation and addition of filler material containing critical raw materials as Cr, Ni and Mn when the following welding parameters are set: current 200 A, welding speed 9,1 cm/min, heat input 1,2 kJ/mm and specific activation flux is used.

1. Introduction

Stainless steel is the name given to a group of corrosion-resistant steels. Stainless steels have a chromium content of at least 10,5 %. The high degree of chromium activity is actually the principal basis for utilizing it as an alloying element in corrosion resisting alloys. As a result of reactions of chromium with the oxygen from the air, a protective oxide film forms on this alloy and prevents further rapid oxidation. Varying additions of Ni, Mo, N, Cu, Mn, W, Ti, Ni and other elements may also be present. [1-6]. Stainless steels are classified on the basis of their matrices as ferritic, martensitic and austenitic stainless steels. Even in the fully soft condition stainless steels have tensile strengths greater than that of mild steel. The soft austenitic steels have exceptional ductility, elongation exceeding 50 %. The austenitic stainless steels can therefore be cold worked to give an extensive range of semi-fabricated and finished products. The cold working may be adjusted so that the final condition attained has the most advantageous combination of strength and toughness. The ferritic stainless steels offer good strength and ductility, but without the outstanding formability of the austenitic varieties.

Duplex stainless steels (DSSs) with austenitic and ferritic grains possess beneficial combinations of these two phases. The ferrite/austenite ratio in DSS must be close to 50:50 by adding appropriate alloying elements for achieving desired microstructures and mechanical properties. DSS exhibit greater toughness and better weldability than ferritic stainless steel [5]. Compared with austenitic grades, DSS have higher resistance to pitting and stress corrosion cracking. Accordingly, they are widely used in various chemical, petrochemical, food, power, transportation, paper and oil industries. Most of these applications require welding as a joining method for parts made from DSS. DSSs undergo

microstructural changes during heat treatment, welding process and prolonged engineering service at high temperatures [5]. In the welding of DSS, it is essential to maintain a ferrite–austenite ratio close to 50:50. This phase balance, may however, be upset due to rapid cooling involved in most weld thermal cycles resulting in weld metal ferrite contents in excess of 50 %. The resultant phase ratio is dependent on the energy input during welding, as this determines the cooling rate and the extent of the phase transformation which is diffusion based. If high heat inputs are used, coarse grains are produced in the weld region, wide heat-affected zones and possibly, precipitation of brittle intermetallic phases may develop [6].

Tungsten inert gas (TIG) welding is a widely used technology for joining stainless steels. When conventional TIG welding process is applied for thick sections it has some disadvantages as low penetration and small deposit, and consequently reduced productivity compared to the other welding processes. Material thickness greater than 3 mm is necessary to weld in multiple passes and this greatly reduces productivity of the process.

One variety of TIG is welding with activation flux coating (A-TIG) on the upper surface of the plates that should be joined. Activating flux is a mixture of inorganic material suspended in an evaporative medium. A thin layer of flux is applied on the surface of the joint before welding [7]. One interpretation is that activating flux influences on the penetration with changing the surface tension in the weld pool so that the fluid flow is opposite of conventional TIG, and tends to increase the penetration [7].

International standard ISO 9692-1:2013 “Welding and allied processes - Types of joint preparation - Part 1: Manual metal-arc welding, gas-shielded metal-arc welding, gas welding, TIG welding and beam welding of steels” gives a recommendation for edge preparation according to the thicknesses of parts to be welded (figure 1). According to this standard for TIG welding of steels in thicknesses $3 < t \leq 8$ mm edge preparation should be square groove with gap between plates $b \approx t$, where t is the thickness of the plate (figure 1.a). Edge preparation for thicknesses $3 < t \leq 10$ should be single V groove with root gap $b \leq 4$ and a V groove angle $40° \leq \alpha \leq 60°$ (figure 1.b). It is notable that edge preparation requires material loss prior the welding and additional filler material during the welding. A-TIG technology makes it possible to intensify the conventional TIG practices for joining the thickness of 8 - 10 mm by single pass full penetration welds, with no edge preparation [7]. In A-TIG welding penetration is increased with the application of a thin coating of activating flux material on the work piece surface prior to welding. The effect of flux is to constrict the arc which increases the current density at the anode root and the arc force on the weld pool. With A-TIG technology the edge preparation is simplified, loss of the material and additional filler material are avoided.

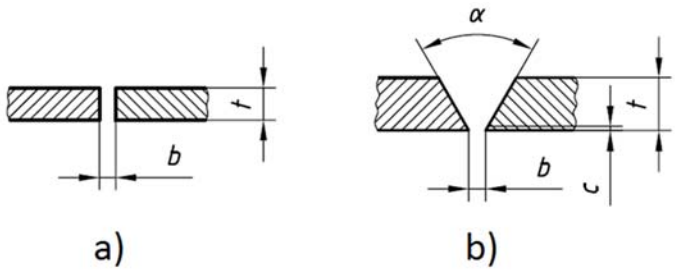

Figure 1. Joint preparation for TIG welding of steels according to the ISO 9692-1:2013

General objective of this research was to clarify the improvements in productivity when TIG welding is applied with activation flux on austenitic-ferrite (duplex) 7 mm thick stainless steel. In the first part specific type of the activation flux has been prepared and the influence on the penetration in bead on plate welding has been examined. According to the achieved penetration parameters for welding two butt joints have been produced with variable shielding gases. Welded joints have been subjected to visual control and destructive tests to verify the validity of the welding parameters.

2. Experimental

2.1 Material

Standard duplex stainless steel with designation X2CrNiMoN22-5-3 has been used in this experiment. Mechanical properties of this material according to the standard HRN EN 10088-2:2015 [8] are presented in table 1. Chemical composition of the same material has been analysed with Energy-dispersive X-ray spectroscopy (EDS) on scanning electron microscope Tescan Vega TS5136 [9]. The results are presented in table 2. The X2CrNiMoN22-5-3 is austenitic-ferritic stainless steel with:

a) high resistance to stress corrosion cracking (SCC) in chloride-bearing environments and environments containing hydrogen sulphide;
b) high resistance to general corrosion, pitting and crevice corrosion;
c) high resistance to erosion corrosion and corrosion fatigue;
d) high mechanical strength - roughly twice the proof strength of austenitic stainless steels;
e) physical properties that offer design advantages;
f) good weldability.

Activation flux has been prepared from powders SiO_2 and Cr_2O_3 in proportion 1:1. In order to prepare highly concentrated powder suspensions 96 % ethyl alcohol has been added in proportion 1:2 to this mixture.

Table 1. Mechanical properties of duplex stainless steel X2CrNiMoN22-5-3 [8]

Thickness [mm]	Yield stress min. $R_{p0,2}$ [MPa]	Tensile strength R_m [MPa]	Elongation min. A [%]
7	460	640 to 840	25

Table 2. Chemical composition of duplex stainless steel X2CrNiMoN22-5-3 [9]

C	Mn	P	S	Si	Ni	Cr	Mo	N
0,014	1,903	0,026	0,002	0,278	5,005	22,421	2,559	0,1690

2.2 Penetration of the electric arc

Penetration of the electric arc has been tested on the test coupons in dimensions 200 × 200 × 7 mm. Plates were cleaned with acetone prior deposition of the activation flux. One thin layer of activation flux was laid on the surface of the work-piece using a paintbrush prior each A-TIG bead on plate welding. Welding was performed with FRONIUS MagicWave 2200 Job G/F TIG welding machine. Thoriated Tungsten electrode with diameter 2,4 mm and designation WT20 has been used for welding. In order to have a linear motion of the electric arc with accurate speed of moving a TIG welding torch has been installed on the „BUG-O Systems“ Modular Drive Systems automatic machine used for guidance in welding. Two types of shielding gas have been used with the same flow of 9 l/min. First of them was 100 % Argon 4.8 (with a purity of 99,998 %) and the other one was a mixture of 97,5 % Argon with 2,5% Nitrogen. Nitrogen has been added to stimulate occurrence of austenitic phase and prevent ferritization. The electrode tip workpiece distance was constantly at 3 mm. Table 3 presents welding parameters for all weld runs in the first part of the experiment. Heat input is defined with the equation:

$$Q = \frac{k \times U \times I \times 60}{v \times 10000} \text{ [kJ/mm]}$$

where U is voltage, I is current, v is welding speed and k is the coefficient of thermal efficiency of the specific welding process (for TIG it is 0,6).

Table 3. Welding parameters in bead on plate welding [9]

Sample	Activation flux	Shielding gas	Welding speed [cm/min]	Current [A]	Voltage [V]	Heat input [kJ/mm]
1A	NO	100 % Ar	10,2	160	11,8	0,666
2A	NO	100 % Ar	7,8	200	13,1	1,209
3A	YES	100 % Ar	10,2	160	13,5	0,762
4A	YES	100 % Ar	7,8	200	14,2	1,310
1B	NO	Ar + 2,5 % N_2	10,2	160	13,6	0,768
2B	NO	Ar + 2,5 % N_2	7,8	200	14,3	1,320
3B	YES	Ar + 2,5 % N_2	10,2	160	13,7	0,774
4B	YES	Ar + 2,5 % N_2	7,8	200	14,8	1,366

2.3 A-TIG welding parameters

After welding and examination of bead on plate welds, parameters for welded joint have been determined. The constant parameters were:

- welding speed 9,1 cm/min;
- shielding gas flow 9 l/min;
- electrode tip workpiece distance 3 mm;
- tungsten electrode diameter 2,4 mm;
- welding torch inclination 90°.

Two welded joints have been produced without any filler material, first one with 100 % Ar shielding gas (marked as Z1) and the other one with Ar + 2,5 % N_2 shielding gas (marked as Z2). Plates in dimensions 200 x 100 x 7 mm were placed on a 10 mm thick cooper backing plate. Plates had single square edge preparation without any spacing between. Samples have been welded with application of the same activation flux in width of 20 mm on the upper surface. Table 4. Presents welding parameters used for producing welded joints.

Table 4. Welding parameters used for producing welded joints [9]

Sample	Activation flux	Shielding gas	Welding speed [cm/min]	Current [A]	Voltage [V]	Heat input [kJ/mm]
Z1	YES	100 % Ar	9,1	200	14,7	1,163
Z2	YES	Ar + 2,5 % N_2	9,1	200	15,4	1,218

2.4 Preparation of samples for analysis

From the produced welds specimens for tensile strength testing, and macrostructure analysis have been sectioned perpendicular to the welding direction using a circular band saw. Specimens for tensile strength test have been machined to required dimensions using a universal milling machine according to the requirements of the standard HRN EN ISO 4136:2013.

Specimens for analysis of macrostructure have been grinded and polished using sandpapers: 1) P320, 2) P500, 3) P1000, 4) P2000 and 5) P4000. After polishing the specimens were etched for 40 s in reagent composed of NaOH and H_2O in proportion 2:3 and using DC current with voltage 2 V.

Specimens for corrosion resistance analysis according to standard ASTM G48-03 (method – A) have been plasma cut in dimensions 100 × 45 mm and washed with hot water to eliminate grease and impurities from the surface.

3 Results

3.1 Visual control

During welding with active flux, the weld pool was calm as it is characteristic for the TIG welding process. There were no spatters on the surface of the material around the produced welds. Sample 1A

has a wider bead on the plate weld in comparison with sample 3A. Heat affected zone and the root of the weld are wider on the sample 3A in comparison with sample 1A. Welds produced with higher current (samples 2A and 4A) have the same influence of the A-TIG welding on the width of the bead on the plate weld. Sample 4A has sufficient penetration on the root side and narrower bead on plate width in comparison with sample 2A that is without root penetration. The difference between samples made with the second shielding gas (Ar + 2,5 % N_2) is the same as with 100 % Ar.

Figure 2 presents weld face and weld root on Z1 specimen. Figure 3 presents weld face and weld root on Z2 specimen. Appearance of the weld on the face side on both samples is very similar and depends only on the guidance of the electric arc. At the root side of the specimen Z1 lack of fusion can be observed after a few centimetres of a correct joint. The reason can be in the incorrect guidance of the electric arc after half of the path. At the root side of the specimen Z2 full penetration can be observed.

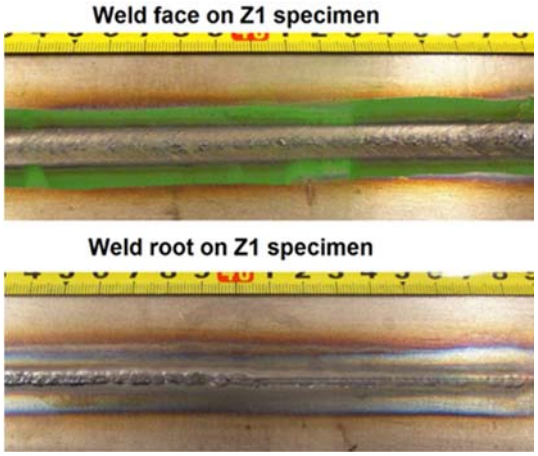

Figure 2. Weld face and weld root on Z1 specimen [9]

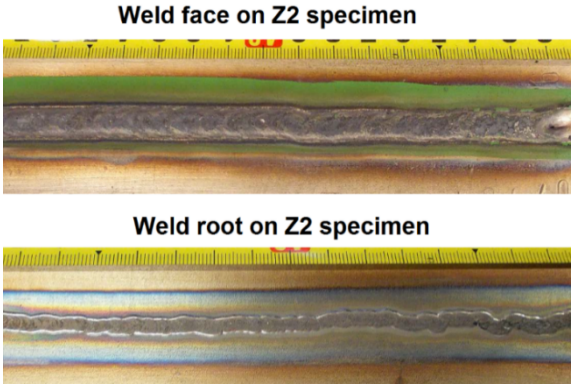

Figure 3. Weld face and weld root on Z2 specimen [9]

3.2 Macrostructure analysis

Macrostructure has been examined on a LEICA MZ6 stereomicroscope, using Leica Application suite version 3.2.0 software. Figure 4 presents a comparison of geometrical features in the produced bead on plate welds in the first part of the experiment. Samples made with 100 % Ar shielding gas are located on the left and samples made with Ar + 2,5 % N_2 are located on the right side of the figure 4. The difference of the geometrical features in dependence on the shielding gas type is clearly seen. When Ar + 2,5 % N_2 has been used, the produced bead on plate welds have wider and shallower penetration in comparison with 100 % Ar shielding gas. Sufficient penetration through the whole thickness has only been achieved when welding current was 200 A and welding speed was 7,8 cm/min.

Figure 5 presents geometrical features of the produced welds Z1 and Z2. Both welds have a minimal face and root reinforcement but have proper shape. Specimen Z1 has a face width 8,1 mm and root reinforcement 0,3 mm. Specimen Z2 made with Ar + 2,5 % N_2 has a smaller face width, 7,6 mm and the root reinforcement 0,4 mm. Transition from an elongated base metal microstructure (obtained with forming of the sheets) to the weld metal microstructure is clearly seen on both welds. It is also possible to see molten metal flow contours from the outside to the inside. This feature is a clear footprint of the Marangoni's effect.

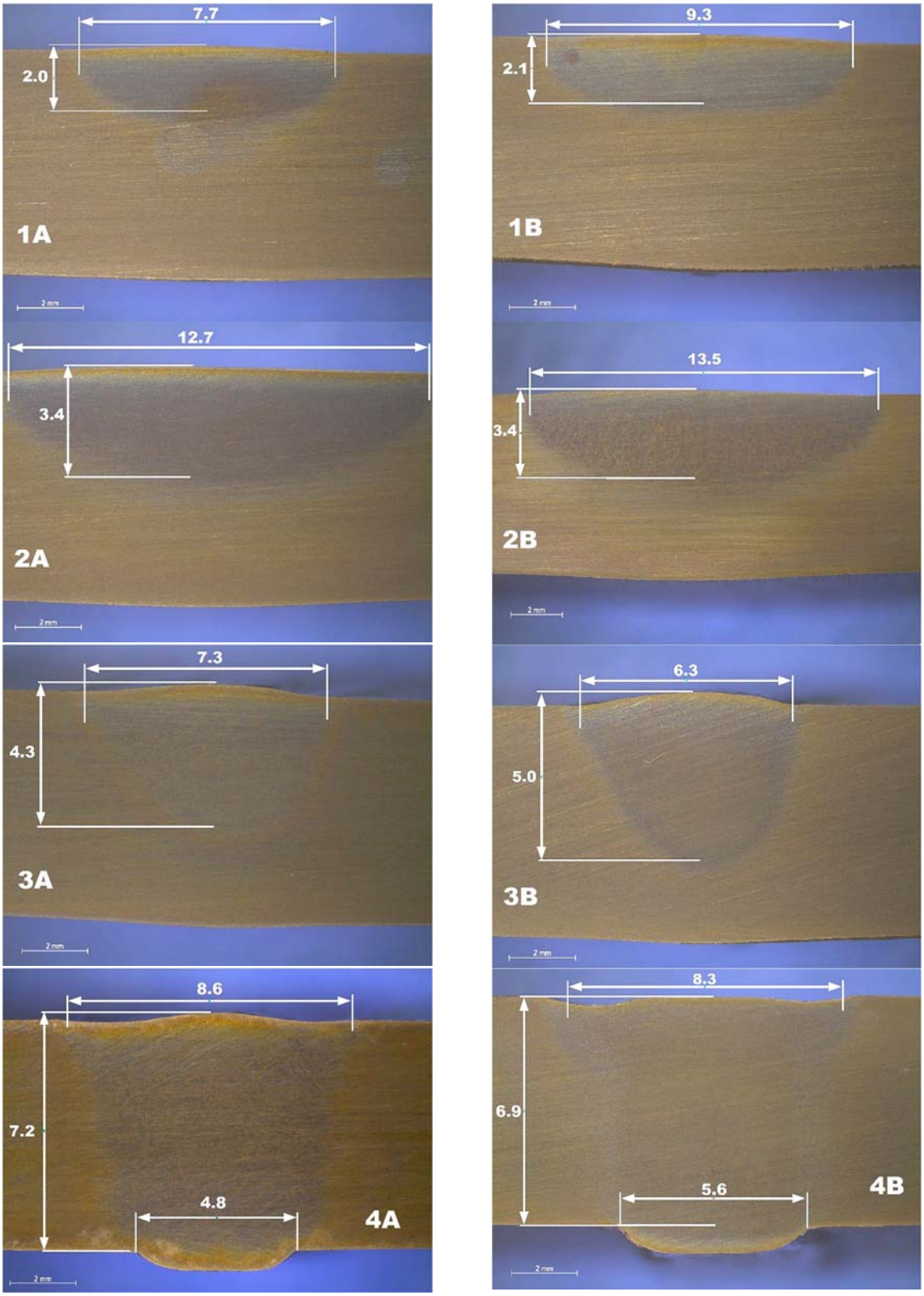

Figure 4. Comparison of geometrical features in the produced bead on plate welds

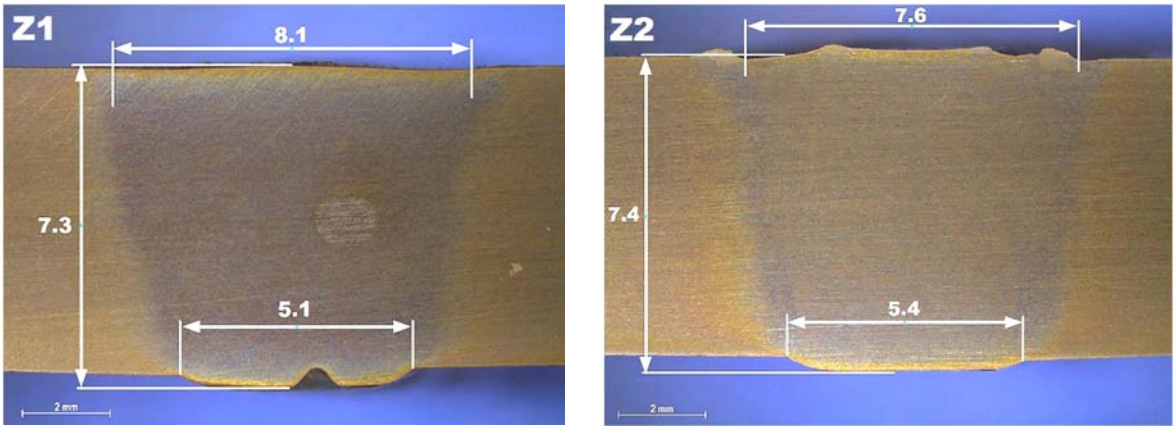

Figure 5. Geometrical features of the produced welds Z1 and Z2

3.3 Tensile strength testing

The uniaxial tensile testing of the specimens has been conducted according to HRN EN ISO 4136:2013 standard [10]. Figure 6 presents samples after the tensile strength testing. Sample Z1 welded with 100 % Ar shielding gas has a fracture in the heat affected zone. Sample Z2 welded with mixture shielding gas 2,5 % N_2 and 97,5 % Ar has a fracture in the base material approx. 40 mm far from the weld centre. Table 5 presents results of the transversal tensile strength testing of the produced welds. From the measured results (table 5) it can be clear that both welds have similar mechanical properties. Measured mechanical properties of the produced welds also fulfil requirements of the HRN EN 10088-2:2015 [8] standard for the base material.

Figure 6. Testing samples after transversal tensile testing [9]

Table 5. Results of the transversal tensile strength testing of the produced welds [9]

Sample	R_m [N/mm^2]	F_m [N/mm^2]	$R_{p0,2}$[N/mm^2]	F_e [kN]	S_0[mm^2]	F_b [kN]
Z1	773,23	136,63	679,12	120	176,70	70,27
Z2	776,45	138,65	683,21	122	178,57	85,29

3.4 Corrosion resistance analysis

Corrosion resistance analysis of the produced welds has been conducted according to the standard ASTM G48 - 03 “Standard test methods for pitting and crevice corrosion resistance of stainless steels

and related alloys by the use of ferric chloride solution "(method A - Ferric chloride pitting test) [11]. Samples were immersed in 10% solution of $FeCl_3$ in H_2O with a temperature of 50°C for a period of 48 h. Figure 7 presents samples after corrosion analysis. It can be observed that most of the pits have been developed in the weld metal on samples 1A, 3A and 4A. Weld metal on sample 2A is free of any pits. Samples welded with mixture shielding gas 2,5% N_2 and 97,5% Ar (1B, 2B, 3B and 4B) are free of pits in the weld metal and the heat affected zone. However, some pits occurred in the base material a few millimeters away from the heat affected zone. A-TIG welding resulted with less pits (3B and 4B) in comparison with conventional TIG welding (1B and 2B).

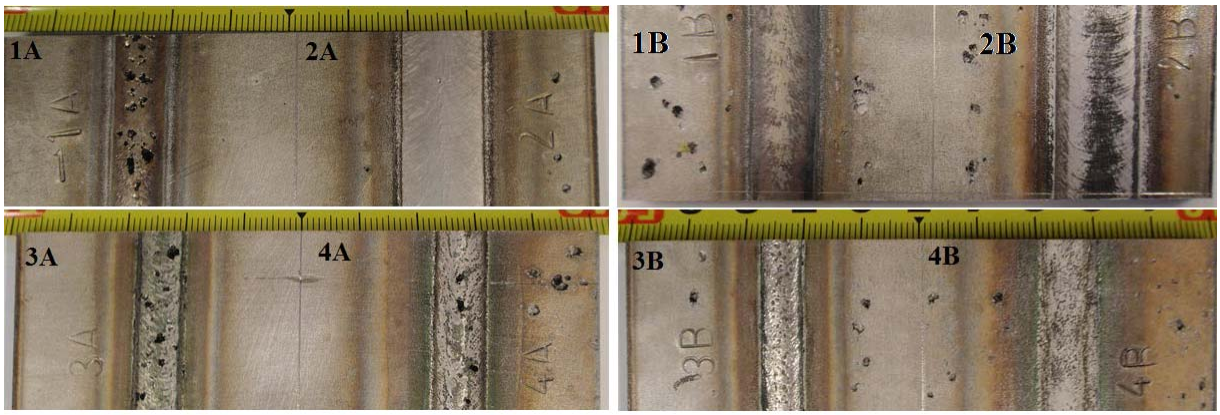

Figure 7. The appearance of bead on plate welds after 48 hours exposure in aggressive solution [9]

4 Conclusions

From the obtained results in this investigation the following conclusions can be summarized:

a) When comparing bead on plate width A-TIG welding produces narrower welds in comparison with conventional TIG. The same influence is observed when welding with current 160 A and with 200 A.
b) Appearance of the weld on the face side of samples welded with A-TIG and conventional TIG welding is almost the same and depends only on the guidance of the electric arc.
c) Macrostructure analysis of geometrical features of the produced bead on plate welds has confirmed that A-TIG welding intensifies the penetration and produces narrower and deeper welds. Shielding gasses used in this experiment have small influence on the geometrical features of the produced welded joints. Full penetration has been achieved only in A-TIG welding with 200 A and with welding speed 7,8 cm/min.
d) Transversal tensile testing of the produced welds has confirmed that both shielding gases influence similar on the tensile strength. Measured mechanical properties of the produced welds fulfill requirements of the standard EN 10088-2:2015 for the base material.
e) Corrosion resistance analysis of the produced welds has confirmed a positive effect of mixture shielding gas 2,5 % N_2 and 97,5 % Ar (1B, 2B, 3B and 4B) on increasing resistance to pitting and crevice corrosion. Bead on plate welds made with mixture shielding gas were free of any pits in weld metal and heat affected zone. A-TIG bead on plate welding resulted with less pits (samples 3B and 4B) in comparison with conventional TIG welding (samples 1B and 2B).
f) A-TIG welding is fully applicable technology for welding butt joint of duplex stainless steel in thickness 7 mm, with mixture shielding gas 2,5 % N_2 and 97,5 % Ar, welding speed and current and other constant parameters according to this experiment.

References

[1] Umoru L E, Afonja A A and Ademodi B Corrosion study of AISI 304, AISI 321 and AISI 430 stainless steels in a tar sand digester, *Journal of Minerals & Materials Characterization &*

Engineering, vol. 7, no.4, pp 291-299, 2008.
[2] Otokumpu Stainless AB *Handbook of Stainless Steel*, Avesta Resarch Centre, Avesta, Sweden, 2013.
[3] Davis J R *Stainless steels*; ASM International, USA, 1994.
[4] Gun R N *Duplex stainless steels: microstructure, properties and applications*; Woodhead Publishing: Cambridge, UK, 1997.
[5] Chan K W and Tjong S C Effect of secondary phase precipitation on the corrosion behavior of duplex stainless steels, *Materials*, no. 7, pp. 5268-5304, 2014.
[6] Gideon B, Ward L and Biddle G Duplex stainless steel welds and their susceptibility to intergranular corrosion*, Journal of Minerals & Materials Characterization & Engineering*, vol. 7, no.3, pp 247-263, 2008.
[7] Shyu S W, Huang H Y, Tseng K H and Chou C P Study of the performance of stainless steel A-TIG welds, *Journal of Materials Engineering and Performance*, vol. 17, no. 2, pp 193-201, 2008.
[8] HRN EN 10088-2:2015, Stainless steels -- Part 2: Technical delivery conditions for sheet/plate and strip of corrosion resisting steels for general purposes
[9] Babić N *A-TIG welding of duplex steels*, Diploma thesis, University of Zagreb, Faculty of Mechanical Engineering and Naval Architecture, 2016.
[10] HRN EN ISO 4136:2013, Destructive tests on welds in metallic materials – Transverse tensile test
[11] ASTM G48 – 03 - Standard test methods for pitting and crevice corrosion resistance of stainless steels and related alloys by use of ferric chloride solution